Mobility of the Surface and Interior of Thin Films Composed of Amorphous Polyethylene

Pemra Doruker and Wayne L. Mattice*

Institute of Polymer Science, University of Akron, Akron, Ohio 44325-3909

Received May 4, 1998; Revised Manuscript Received November 5, 1998

ABSTRACT: We performed coarse-grained simulations of thin polyethylene films of different thicknesses at 509 K. The films, which present two surfaces to vacuum, are formed from monodisperse melts of $C_{100}H_{202}$. The mobility increases toward the free surfaces at the scale of individual beads and chains due to the decrease in density. The diffusion of the chains parallel to the surfaces increases as the film thickness decreases. In contrast, the diffusion in the direction normal to the surfaces slows down as the film thickness decreases. This slowing down seems to be primarily a result of the confinement of the chains between the surfaces.

Introduction

It is known experimentally that the mobility of polymer chains may be substantially altered near a surface or interface. Recently, several experiments[1−7] were performed with thin polymer films supported on surfaces. There are contradictory results on whether the chain mobility (or the glass transition temperature) increases/decreases or does not change at free surfaces. In these experiments, there are two different boundaries, i.e., a polymer−vacuum and a polymer−solid boundary. It is difficult to determine how the different boundaries affect the mobility of chains independent of each other in setups where both of the boundaries exist. Moreover, the results are affected by the strength of the interactions between the polymer and the solid surface. Forrest et al.[8] measured the glass transition temperature of free-standing films with polymer−vacuum boundaries on both sides. They used polystyrene films with varying thicknesses and showed that the glass transition temperature decreases with decreasing film thickness.

Simulations have been helpful in analyzing systems that contain either vacuum or solid boundaries. Specifically, Mansfield and Theodorou[9] showed by molecular dynamics simulation that the local mobility on the nanosecond time scale was enhanced at the free surfaces of a glassy atactic polypropylene film. The length scale for this enhancement in mobility due to the polymer−vacuum interface was larger than the radius of gyration of the polymer chains. In Monte Carlo studies of a confined, coarse-grained polymer melt, Baschnagel and Binder[10] showed the displacement of monomers and the centers of mass of coarse-grained polymer chains increased in the parallel and decreased in the perpendicular direction at the polymer−wall interfaces.

In this study, we will analyze the local and whole-chain dynamics of free-standing polyethylene (PE) melt films using Monte Carlo simulations on a high coordination lattice, which is called the second-nearest-neighbor diamond (2nnd) lattice. This lattice is formed by connecting every other lattice site on a diamond lattice.[11] It was introduced for the simulation of rotational isomeric state (RIS) model polymer chains at bulk density.[12−18] Simulation of bulk PE was successful on the 2nnd lattice, after the incorporation of short-[12] and long-range[14,15] interactions. During the course of this specific Monte Carlo simulation, it is also possible to reverse-map any coarse-grained snapshot back to the atomistic model in continuous space by placing the missing atoms on the lattice and performing energy minimization on the system.[15] Thus, large bulk and film systems can be equilibrated efficiently, and further atomistic simulations or analysis of the snapshots in continuous space can be performed.

In recent work, PE thin films were formed on the 2nnd lattice, and the static properties of the equilibrated films were investigated.[17] The surface energies obtained from the simulations were close to experimental data. Major findings of this study[17] can be summarized as follows: (i) Films of different thicknesses, i.e., consisting of different number of chains, exhibit almost identical hyperbolic density profiles at the interface. (ii) The end beads are predominant and the middle beads are depleted at the free surfaces. (iii) There is anisotropy in the orientation of bonds and chains at the interface. (iv) The center-of-mass distribution of the chains exhibits oscillatory behavior across the films. In this study, we will analyze the dynamic properties of these films in detail to provide more insight about the mobility of thin films. Specifically, the local and global mobility of chains in thin films with different thicknesses will be studied and compared to bulk simulations.

Simulation Details

The 2nnd lattice sites are identical to the hexagonal packing of hard spheres. However, we identify it as the "2nnd lattice" in order to refer to the original diamond lattice, which serves as a useful medium to map several RIS model chains. It has a coordination number of 12. Details about this lattice can be found in refs 11 and 12. In the case of PE chains, each lattice site can accommodate a CH_2CH_2 unit (or a CH_2CH_3 unit at the chain ends).

The short-range interactions, which determine the local conformational preferences of specific polymer chains on the lattice, are modeled by using the RIS formalism.[19,20] The original RIS model for PE developed by Abe et al.[21] is mapped unto the coarse-grained 2nnd lattice. Details for this procedure can be found in ref 12.

10.1021/ma9807015 CCC: $18.00
Published on Web 12/16/1998

Long-range intra- and intermolecular interactions among nonbonded units are derived from the Lennard-Jones potential for ethylene units. An average interaction energy is assigned for each neighboring shell around a lattice site by using the second virial coefficient expression. Details for the determination of average long-range energies can be found in ref 14. Self- and mutual avoidance is applied to all beads. Here, we use the parameter set II in ref 17, which is found to produce reasonable density in the bulk region of PE thin films. The average interaction energies for the first three shells are 14.122, 0.526, and −0.627 kJ/mol, sequentially.[17] The attractive third-shell interaction energy brings cohesion to the system. Thus, it is possible to perform thin-film simulations on the 2nnd lattice. Thin films are generally formed by using equilibrated bulk snapshots and increasing one periodic side of the system to infinity. However, another method, where two films are healed to increase the system size, can also be used. Details about the different procedures of film formation are given in ref 17. Both methods lead to films with identical properties after proper equilibration periods.[17]

Single bead moves are performed in the simulations. Each move corresponds to the displacement of two or three backbone atoms on the fully atomistic PE chain. Each Monte Carlo step (MCS) corresponds to a series of single bead moves, where all the beads in the system are randomly attempted for movement. Details on the different kinds of single bead moves allowed in the simulations are given in ref 15. Since only local moves are allowed in the simulations, the dynamics of bulk PE systems were found to be satisfactory[22] when compared with results from conventional fully atomistic molecular dynamics simulations.[23]

PE chains simulated on the 2nnd lattice are made of 50 coarse-grained beads (CH_2CH_2 units), which correspond to $C_{100}H_{202}$ after reverse mapping. Two films of different thicknesses are formed, which consist of either 36 or 72 chains. The films present two free surfaces to vacuum. The periodic cross-sectional area of all films in the X and Y directions is 2501 Å^2 (21 × 22 lattice sites with 2.5 Å lattice spacing). The film thickness in the Z direction (normal to the free surfaces) varies according to the number of chains in the system, since the system chooses its own bulk density due to cohesive long-range interactions. Simulations are performed for 2×10^6 MCS after equilibration periods of $(2-3) \times 10^6$ MCS. We will mainly present the results from the thin-film melts at 509 K, which will be differentiated by the number of chains as f36 and f72. For comparison, a bulk simulation is performed with 32 chains of the same chain length in a periodic box of 21 × 21 × 22 lattice sites at 509 K, which has a density of ∼0.7 g/cm^3, comparable to the density in the interior of the thin films.

Results and Discussion

Density Profiles vs Acceptance Rates. The density profiles of the two films at 509 K are presented in Figure 1a, where $Z = 0$ denotes the center of mass of the films on the axis that is normal to the two melt−vacuum interfaces. The interfacial profiles of f72 (solid line) and f36 (dashed line) are almost identical. (See ref 17 for details on the equilibrium properties of these films.) The films are divided into bins of 6 Å width, starting from $Z = 0$, to view the differences between the dynamics of the bulk and interfacial regions. This bin size is approximately half the root-mean-square radius of gyration of the chains in the film. The vertical grids, which are numbered on the top of the figure, represent the bins that will be used in the following discussion. Looking at the density profile of the thicker f72 film, bins 1−6 and 7−10 correspond to the bulk and interfacial regions, respectively, as defined by the density profile.

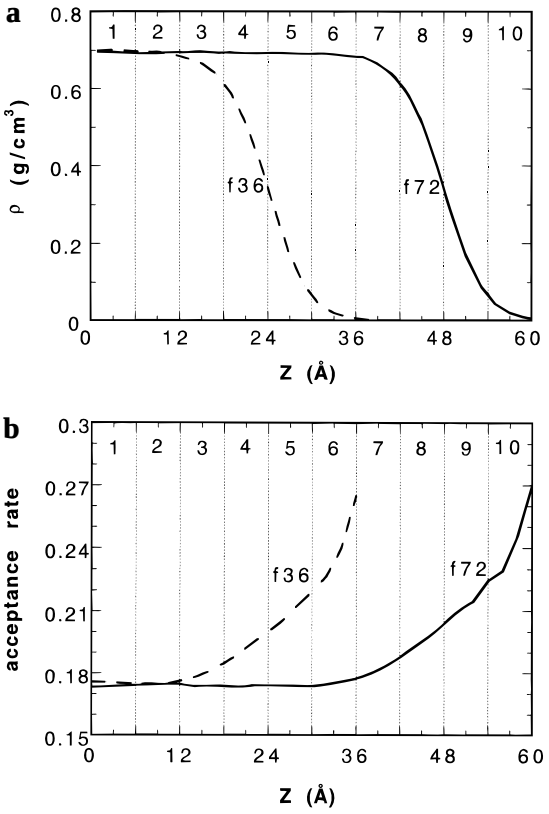

Figure 1. (a) Density profiles of two films from the center of mass of the film in the Z direction, which is normal to the free surfaces. The vertical bins indicate the cross sections over which averaging is done for analysis. (b) Acceptance rate of the single bead moves across the same films.

In Figure 1b, the acceptance rate of the single bead Monte Carlo moves is shown as a function of the Z coordinate from the film center of mass. The ordinate denotes the number of accepted moves divided by the number of total attempted moves on the beads that lie on a specific lattice plane with a constant Z coordinate. The mobility of the beads increases as the density decreases at the interface. The acceptance rate of ∼17.5% at the center of the films is identical to the value in bulk simulations, carried out at a density of 0.7 g/cm^3.

Mobility of Beads and Chains. Figure 2 shows how long the middle beads of the chains in the f72 film reside in their original bin. The ordinate gives the fraction of beads that stay in the same bin as a function of MCS, i.e., time. The beads starting out in bins 1−6 (the bulk region) exhibit almost identical decay, whereas the residence time decreases as the bin number increases toward the free surface. The same trend is observed in the case of end beads of the chains (not shown). However, end beads have a higher mobility compared to the middle beads, as expected. Similarly, Figure 3 shows the fraction of chains that stay in the same bin as a function of MCS, by looking at the center of mass of each chain. This figure for film f72 shows the mobility of the chains in the Z direction, specifically. The chains

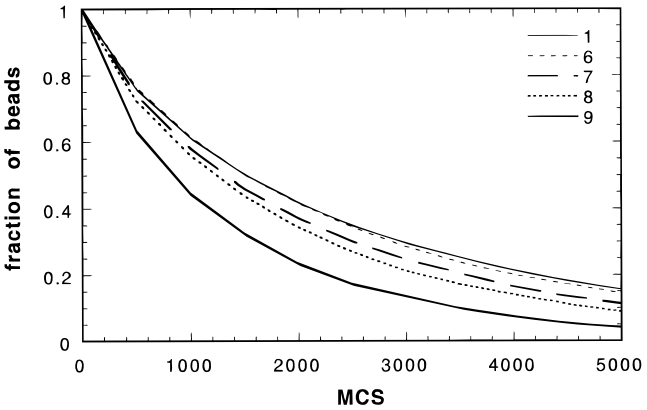

Figure 2. Fraction of middle beads (of the chains in film f72), which stay in their original bin, as a function of MCS.

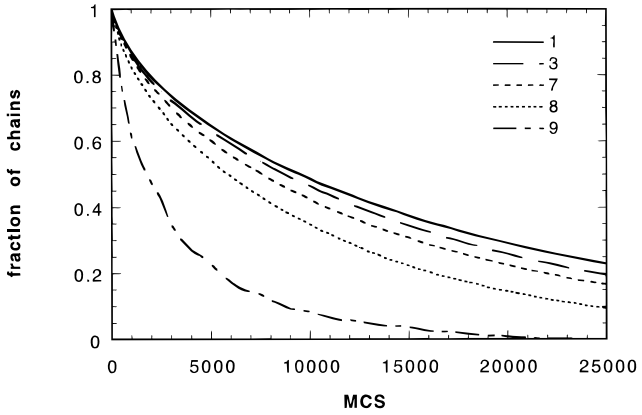

Figure 3. Fraction of the centers of mass of polymer chains in film f72, which stay in their original bin, as a function of MCS.

in the innermost bulk region (bins 1−3) have a longer residence time compared to the chains on the vacuum side of the interface (bins 8 and 9). The mobility of the chains in the Z direction is progressively increasing toward the interface, starting from the bulk region. Thus, the effect penetrates into the bulk region (bins 1−6) as well, when the mobility of chains is considered. In contrast, the increase in mobility of beads is only effective in the interfacial region (bins 7−9). The chains in the thin film have a root-mean-square radius of gyration of 13 ± 1 Å, and therefore an appreciable fraction of the beads in bins 7−9 belong to chains with their center of mass located in bins in the interior of the film. Movement of these beads will affect the coordinates of the center of mass in the interior of the film. In summary, Figures 2 and 3 indicate that the mobility increases toward the free surface at the level of individual beads and chains.

Rotational Diffusion of the Chains. Figure 4 gives the normalized end-to-end vector autocorrelation function as a function of MCS for the f72 film. There is a gradual decrease in the decorrelation time with increasing bin number in the bulk region of the film (bins 1−6) and a fast decrease in the interfacial region (bins 7−9). The rotational diffusion of the chains is also enhanced in the region of lower density at the interface.

Translational Diffusion of the Chains. The free surfaces impose anisotropy on the center-of-mass displacement of the chains. Therefore, the lateral (average of X and Y directions parallel to the surface) and perpendicular (Z direction, normal to the surfaces)

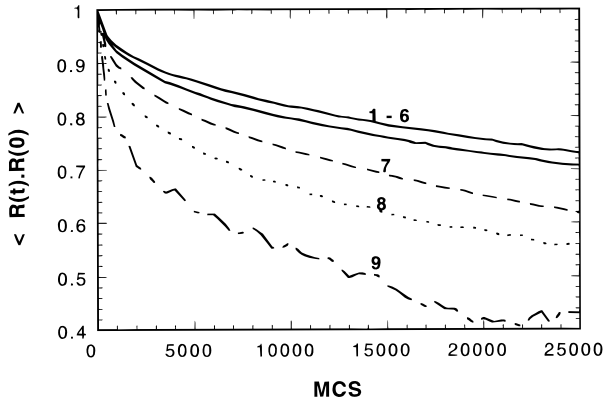

Figure 4. Normalized end-to-end vector autocorrelation function of the chains starting in different bins, as a function of MCS, for film f72.

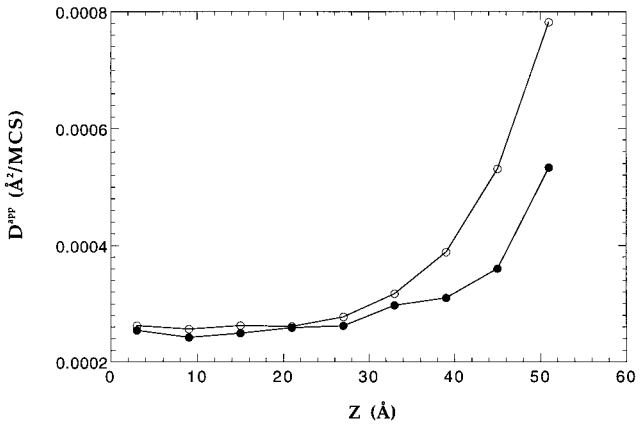

Figure 5. Apparent diffusivity in different bins across the f72 film (see text for definition). Empty and filled circles indicate D_{XY}^{app} and D_Z^{app}, respectively, for t_f = 5000 MCS.

components of diffusion will be considered separately. "Apparent diffusivity"[24] in the Z direction (normal component) can be calculated as

$$D_Z^{app} = (1/2t_f)\langle[Z_{c.m.}(t+t_f) - Z_{c.m.}(t)]^2\rangle \qquad (1)$$

Here, $Z_{c.m.}$ is the Z coordinate of the chain center of mass and t_f is an arbitrary final time. We can choose t_f such that the chains in different bins can still be differentiated. Referring to Figure 3, t_f = 5000 MCS seems to be suitable for this purpose, since at least 50% of the beads in each bin stay in the same bin during this time period, except for the outermost bin 9. The apparent diffusivity parallel to the surfaces, D_{XY}^{app}, is calculated using the same equation and averaging over the center-of-mass displacements in the X and Y directions. In Figure 5, the empty and filled circles indicate D_{XY}^{app} and D_Z^{app}, respectively, which are calculated using t_f = 5000 MCS. The data points are averages within each bin from 1 to 9. The diffusion is enhanced toward interface, in both parallel and normal directions to the surface. However, the increase in the parallel direction is much greater. The bulk value of diffusivity reached in the middle of the film is comparable to the value of 2.68×10^{-4} Å²/MCS, which is obtained from the bulk simulation carried out at a density of ∼0.7 g/cm³. The deviations in the apparent diffusion coefficient from the bulk value due to the presence of the free surface are not restricted to the interfacial region but penetrate into the bulk region, as well. An almost identical trend is obtained at the interface of f36 (not shown).

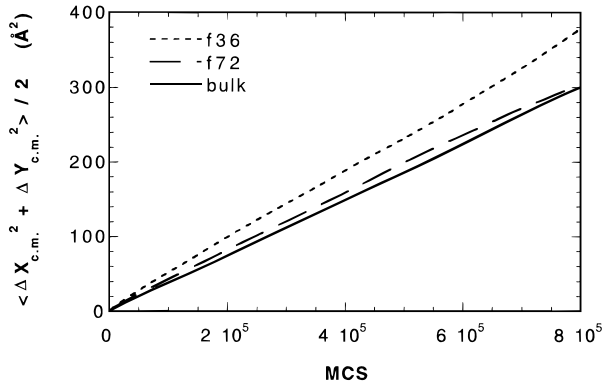

Figure 6. Squared center-of-mass displacement averaged in *X* and *Y* directions as a function of MCS. The *XY* plane is parallel to the surface of the films and arbitrary in the bulk simulation.

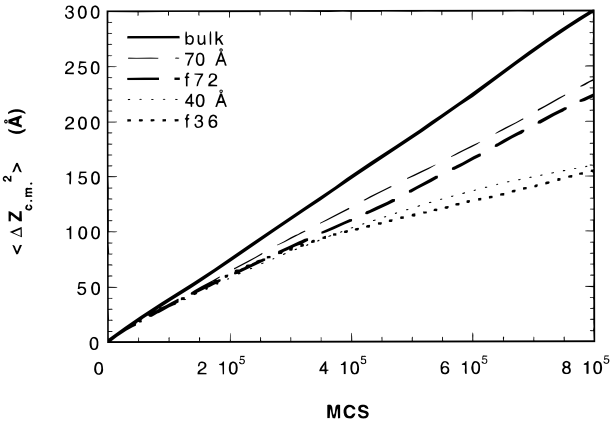

Figure 7. Squared center-of-mass displacement in *Z* direction as a function of MCS. *Z* direction is normal to the surface of the films and arbitrary in the bulk simulation.

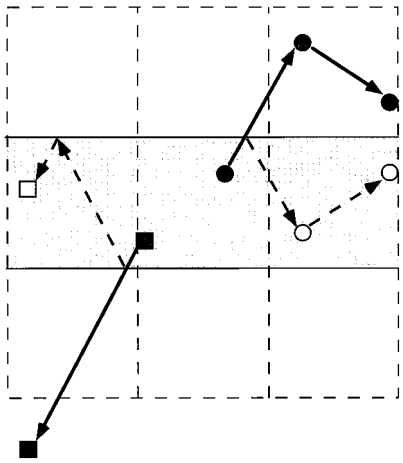

Figure 8. Representation of "reflecting hard walls" analysis using the bulk simulations (see text for details).

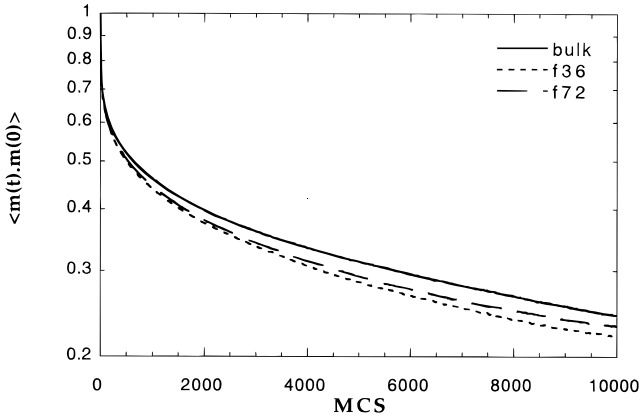

Figure 9. Orientation autocorrelation function of the 2nnd bond vectors, as a function of MCS, for films and bulk.

The apparent diffusivity of the chains gives information on a short time scale, since in the long time limit the chains in different bins can no longer be identified as belonging to a particular bin. Therefore, we also monitored the overall diffusion of all of the chains in the two films (without regard to their position) and compared it with the bulk simulation results. In Figure 6, the squared center-of-mass displacement of the chains averaged in *X* and *Y* directions is plotted as a function of time (MCS) for the films and the bulk simulation. (The *X* and *Y* directions for the bulk are chosen arbitrarily.) The diffusion is higher in the f36 film compared to f72 and bulk simulations. This results from the fact that the interfacial region is dominant in the f36 film, and the lateral diffusion is enhanced in the interfacial region.

Figure 7 gives a similar plot for diffusion in the *Z* direction. The axial diffusion decreases as the film thickness decreases. This slowing down of diffusion in the films compared to the bulk simulation may be due to the confinement in the *Z* direction. We wanted to check this hypothesis by putting some "imaginary" hard walls in one direction of the bulk simulation (periodic in three directions) and then analyzing the trajectories as periodic in two directions, to determine whether confinement effects produced by imaginary walls introduced into a bulk calculation are functionally equivalent to the thin film calculations. Figure 8 illustrates how we perform this analysis. The walls are placed at a spacing of Δd. Any chain, whose center of mass moves out of the gray region, is reflected in the opposite *Z* direction (keeping the same *X* and *Y* coordinates) during the analysis, so that the centers of mass of the chains stay in the gray region all the time. The center-of-mass trajectories of two different chains (squares and circles) are presented in the figure. The real bulk trajectories are traced by solid lines, whereas the modified trajectories for the hard wall analysis are traced by dashed lines. This specific analysis procedure of bulk trajectories mimics a bulk system confined between perfect hard walls, where the centers of mass of the chains barely touch but cannot penetrate the reflecting walls. In Figure 7, the two lines plotted with very thin dashes represent the results from reflecting hard walls analysis with two different Δd values. Here, the mean-squared center-of-mass displacement at $\Delta d = 40$ Å is almost coincident with that of the f36 film simulation, and $\Delta d = 70$ Å coincides with the f72 results. These wall spacings are also close to the thickness of the respective films, as shown by the density profiles in Figure 1a. Therefore, the confinement of the chains between two free surfaces seems to be the predominant reason for the slowing down of the axial diffusion.

The mean-squared radius of gyration of the chains is 180 ± 22 Å^2 in the film simulations. Therefore, the chains move over a distance twice the radius of gyration during the simulation.

Orientation Autocorrelation Function (OACF) of Bond Vectors. Figure 9 displays OACF or the first Legendre polynomial of the 2nnd bond vectors, given

Table 1. Summary of the Relationship between the Mobilities at the Surface and Interior of the Thin Films

surface more mobile than interior	surface less mobile than interior
acceptance rates (Figure 1b)	apparent diffusivity in normal direction at longer time (Figure 5)
residence time of individual beads (Figure 2)	normal component of the diffusion coefficient (Figure 7)
residence time of centers of mass (Figure 3)	
decorrelation of end-to-end vectors (Figure 4)	
apparent diffusivity at short time (Figure 5)	
parallel component of the diffusion coefficient (Figure 6)	
OACF for chord vector (Figure 9)	

by $\langle \mathbf{m}(t)\cdot\mathbf{m}(0)\rangle$, as a function of time. Bond vectors on the coarse-grained lattice correspond to backbone C−C−C chord vectors in the real PE chain. The decorrelation times for the different systems can be ordered as follows: bulk > f72 > f36. Again, the predominance of the surface layer in f36 enhances the decay of the OACF in this system.

Concluding Remarks

The relationship between the mobilities at the surface and interior of the thin films is summarized in Table 1. The necessity for use of two columns in this table shows that the qualitative nature of this relationship depends in an important way on the precise definition of "mobility", even when all of the analysis is performed on exactly the same trajectory.

Most of the definitions employed in this work lead to the conclusion that the surface region is more mobile than the interior of the thin film. The opposite conclusion is obtained if the mobility is defined as the diffusion coefficient (or long-time apparent diffusivity) in the direction normal to the surface.

If the mobility is defined locally (in terms of three consecutive CH_2 units in the fully atomistic representation of the chain), all of our analysis leads to the conclusion that the surface is more mobile than the interior. These definitions use the acceptance rate, residence times of individual beads, and the orientation autocorrelation function for the coarse-grained bond vector (C−C−C chord vector for the fully atomistic model). Although our simulations are performed well above the glass transition temperature for polyethylene, our finding that the surface is more mobile than the interior (when mobility is defined in terms of local motion of very small portions of the chain) is consistent with the glass transition temperature being lower at the surface than in the bulk. The most pertinent experiments are those performed on free-standing thin films of polystyrene.[8] Our simulations of free-standing thin films of PE show qualitatively similar effects. Quantitative comparison is difficult because the polymers are different.

When the mobility is assessed at the level of the entire chain, qualitatively different relationships between the mobility at the surface and in the bulk can be obtained, depending on the exact definition used for the motion of the chain.

These results from the simulation suggest that different experiments, which sense the mobility of the system in different ways, may yield apparently contradictory information about the relationship between the mobility at the surface and in the interior of exactly the same film.

Acknowledgment. This work was supported by Grant DMR 9523278 from the National Science Foundation.

References and Notes

(1) Keddie, J. L.; Jones, R. A. L.; Cory, R. A. *Europhys. Lett.* **1994**, *27*, 59.
(2) Zheng, X.; Sauer, B. B.; van Alsten, J. G.; Schwartz, S. A.; Rafailovich, M. H.; Sokolov, J.; Rubenstein, M. *Phys. Rev. Lett.* **1995**, *74*, 407.
(3) Xie, L.; DeMaggio, G. B.; Frieze, W. E.; DeVries, J.; Gidley, D. W.; Hristov, H. A.; Yee, A. F. *Phys. Rev. Lett.* **1995**, *74*, 4947.
(4) Tanaka, K.; Taura, A.; Ge, S.; Takahara, A.; Kajiyama, T. *Macromolecules* **1996**, *29*, 3040.
(5) Frank, B.; Gast, A. P.; Russell, T. P.; Brown, H. R.; Hawker, C. *Macromolecules* **1996**, *29*, 6531.
(6) Kajiyama, T.; Tanaka, K.; Takahara, A. *Macromolecules* **1997**, *30*, 280.
(7) Liu, Y.; Russell, T. P.; Samant, M. G.; Stîhr, J.; Brown, H. R.; Cossy-Favre, A.; Diaz, J. *Macromolecules* **1997**, *30*, 7768.
(8) Forrest, J. A.; Dalnoki-Veress, K.; Stevens, J. R.; Dutcher, J. R. *Phys. Rev. Lett.* **1996**, *77*, 2002.
(9) Mansfield, K. F.; Theodorou, D. N. *Macromolecules* **1991**, *24*, 6283.
(10) Baschnagel, J.; Binder, K. *J. Phys. I* **1996**, *6*, 1271.
(11) Rapold, R. F.; Mattice, W. L. *J. Chem. Soc., Faraday Trans.* **1995**, *91*, 2435.
(12) Rapold, R. F.; Mattice, W. L. *Macromolecules* **1996**, *29*, 2457.
(13) Doruker, P.; Rapold, R. F.; Mattice, W. L. *J. Chem. Phys.* **1996**, *104*, 8742.
(14) Cho, J.; Mattice, W. L. *Macromolecules* **1997**, *30*, 637.
(15) Doruker, P.; Mattice, W. L. *Macromolecules* **1997**, *30*, 5520.
(16) Bahar, I.; Cho, J.; Erman, B.; Haliloglu, T.; Kim, E.-G.; Mattice, W. L.; Monnerie, L.; Rapold, R. F. *Trends Polym. Sci.* **1997**, 5, 155.
(17) Doruker, P.; Mattice, W. L. *Macromolecules* **1998**, *31*, 1418.
(18) Haliloglu, T.; Mattice, W. L. *J. Chem. Phys.* **1998**, *108*, 6989.
(19) Flory, P. J. *Statistical Mechanics of Chain Molecules*; Wiley: New York, 1969.
(20) Mattice, W. L.; Suter, U. W. *Conformational Theory of Large Molecules. The Rotational Isomeric State Model in Macromolecular Systems*; Wiley: New York, 1994.
(21) Abe, A.; Jernigan, R. L.; Flory, P. J. *J. Am. Chem. Soc.* **1966**, *88*, 631.
(22) Doruker, P.; Mattice, W. L. *Macromol. Symp.* **1998**, *133*, 47.
(23) Paul, W.; Smith, G. D.; Yoon, D. Y. *Macromolecules* **1997**, *30*, 7773.
(24) Yoon, D. Y.; Vacatello, M.; Smith, G. D. In *Monte Carlo and Molecular Dynamics Simulations in Polymer Science*; Binder, K., Ed.; Oxford University Press: New York, 1995; p 433.

MA9807015